ICAS PAPER
NO. 72 – 42

CALCULATION OF THE RECIRCULATION FLOW OF VTOL LIFT ENGINES

by

E. Schwantes, Dr.–Ing.
DFVLR, Institut für Luftsaugende Antriebe
Braunschweig, Germany

The Eighth Congress of the International Council of the Aeronautical Sciences

INTERNATIONAAL CONGRESCENTRUM RAI–AMSTERDAM, THE NETHERLANDS
AUGUST 28 TO SEPTEMBER 2, 1972

Price: 3. Dfl.

CALCULATION OF THE RECIRCULATION FLOW OF VTOL LIFT ENGINES

Dr.-Ing. E. Schwantes

DEUTSCHE FORSCHUNGS- UND VERSUCHSANSTALT
FÜR LUFT- UND RAUMFAHRT E.V.
Institut für Luftsaugende Antriebe

Braunschweig, Germany

SUMMARY

A method is developed to predict theoretically the increase of temperature due to wind-recirculation in the inlet of a VTOL lift engine exhausting normally to the ground. It is shown how to calculate with the potential-theory the velocities in the recirculation flow and how to determine the temperatures with the laws of spread of buoyant plumes. Model-investigations are done to check these results. The model-jets operated with critical nozzle pressure ratio and temperatures up to 1ooo°C.

SYMBOLS

b	width
c_p	heat capacity
D	nozzle diameter
e	basis of natural logarithm
F	area, thrust
g	acceleration due to gravity
Gr	Grashof's number
H	height of nozzle exit above the ground
M	mach number
$\dot{m}$	mass flow
P	pressure
R	radius measured from stagnation point, radius of separation
r	radius, distance
Re	Reynold's number
s	length, standard tolerance
T	temperature
t	time
u	velocity component
V	volume, substitution value
$\dot{V}$	volume flow
v	velocity component

W	substitution value
w	wind velocity
X	force per volume
x	co-ordinate
x'	distance in x-direction
y	co-ordinate
y'	distance in y-direction
Z	substitution value
z	co-ordinate
α	velocity ratio
γ	non-dimensional parameter for temperature gradient
ξ	non-dimensional parameter for upwind velocity
η	non-dimensional parameter for upwind width
θ	excesstemperature compared with ambient temperature, potential temperature
θ'	overtemperature of upwind
λ	non-dimensional parameter for upwind temperature, coefficient of thermal conductivity
μ	dynamic viscosity
ξ	non-dimensional parameter for passage of upwind
ρ	density
ϕ	potential function
φ	angle of rotation

INDICES

o	condition at the nozzle exit
a, ∞	ambient condition
b	width
m	average
max	maximum value, maximum value at axis
W	wind influence

all dimensions are presented in Millimeters

1. INTRODUCTION

The planning and construction of V/STOL*)-aircrafts is considerably influenced by the ground-effects that are induced by the free jet of the lift engines. These effects cause both lift-increases and lift-decreases on the aircraft frame, loss of thrust of the engines by recirculation, destruction of the runway and airframe by ground-erosion and in addition considerable noise pollution. The following jet-induced ground effects can be distinguished:

aerodynamic ground effects
thermic ground effects (recirculation)
  fountain recirculation
  wind recirculation
ground erosion
noise.

At the recirculation, the thermic ground effect, a part of the hot jet is conveyed again by deflection on the ground, by sink-effect of the engine inlet and by thermic buoyancy forces back to the inlet. The sensitive reaction of jet engines to an increase of the compressor-inlet temperature is represented graphically in fig.2, in the example of the lift engine Rolls Royce RB 162-31 (fig.1): two degrees increase of temperature already cause one percent decrease of thrust. The great efforts of engineers to protect engine inlets of VTOL-aircrafts against recirculation flow are therefore fully justified.

If several free jets impinge horizontally on the ground, their wall jets deflect one another in the form of fountains upwards. In this way hot engine exhaust-gases can enter directly the compressor inlets, influence thrust, extinguish the engines or damage the aircraft frame by high temperature. This is called the fountain-recirculation, respectively recirculation of the vicinity. Local temperature peaks up to 7o% of the nozzle temperature have been measured in such gushing up hot gas flows in the engine inlet plane. Not only loss of thrust can be registered, but the performance of the engine is also distorted badly by such asymmetrical temperature profiles in the inlet section (inlet distortion). On the basis of detailed series of experiments during the past years new aircraft designs can nowadays eliminate arrangements that may cause hot gas fountains. Fountains can for instance be avoided by a slight tilt of the engine jet from the vertical position to the ground or by injecting an auxiliary jet that dissipates the fountain.

Today wind recirculation is being regarded more problematic (fig.3). This process - also called the "recirculation of the remote zone" - occurs when a wind flow encounters a propulsion jet that has been deflected on the ground. The wind flow separates the hot wall jet from the ground and conveys it back to the engine inlet. This warm air cloud overflows in adversable cases the complete aircraft.

Contrary to hot gas fountains the wind recirculation causes relatively slight increases of temperature in the inlet only. They seldomly pass 3o°C. On the other hand it is very difficult to control or even eliminate this kind of recirculation. The trend in the lift engine technique to use jets of bigger volume with low specific momentum places the problem of wind recirculation all the more in the foreground. This paper deals exclusively with wind recirculation.

---

*) vertical/short takeoff and landing

2. CALCULATION OF RECIRCULATION VELOCITIES

It is intended to specify a technique that enables a potential-theoretical calculation of the velocity vectors of the complete three-dimensional recirculation flow field around a lift engine that impinges normally on the ground. According to definition potential flows are frictionless flows of constant temperature. Frictionlessness is fulfilled in the recirculation flow field, however there can be no mentioning of an isothermal flow.

As will be shown in the following estimation the differences in temperature in the secondary flow field are small. Therefore the buoyant forces - due to local overtemperatures - are small against the kinetic forces, caused by wind blowing and by the suction effect of the jet. This can be illustrated by the ratio:

$$(1) \qquad \frac{\text{kinetic force}}{\text{buoyant force}} \sim \frac{Re^2}{Gr} \quad .$$

As have been proved in [4] the characteristic ratio is of the order of:

$$8 < \frac{\text{kinetic force}}{\text{buoyant force}} < 13o \quad .$$

In the recirculation flow field the kinetic force exceeds the thermic force by one to two tenth powers. Therefore the kinetic force is the preponderant value for the flow character and allows a potential-theoretical calculation of the recirculation field.

If one superposes a series of sources and sinks appropriately a similar velocity-field can be induced in the neighborhood of the singularities as is caused by a lift engine impinging on the ground. With the potential-theoretical model the secondary flow field is described that is induced by the jet engine and the propulsion jet. The flow conditions in the primary jet and in the adjacent turbulent mixing zone cannot be reproduced by this method. The sink-effect of the engine inlet is produced by two adjacent point-sources and point-sinks of different strength. The suction effect of the free jet and of the wall jet can be simulated by line- and surface-sinks resp.. Light intersection photos of the inflow of the free jet and of the wall jet show that the flow direction of the secondary air into the jet is not normal to the outer surface area of the jet. The inflow direction deviates at the jet boundary from the normal one. Therefore it seems more reasonable to place the line sink that causes the suction effect of the free jet on the jet axis and not on the outer surface area of the jet. The same applies to the surface-sink of the wall jet. The separation of the wall jet from the ground induced by wind and the thermic buoyant forces will be reproduced by the flow that is induced by a source on a cylinder area combined with an adjacent annular sink. Surface singularities always stream to the both sides. On that account the inwardly directed flow of the cylinder source that disturbs the recirculation flow field, has to be absorbed by the annular sink. In [4] it is pointed out that the line of separation directed against the wind is deformed from a circular ring into an ellipse. Therefore elliptical shapes must be introduced in the potential-theoretical model. This applies to the surface-sink that simulates the wall jet and to the source-sink pair that represent the separation; it also applies

to the cylinder sink and to the annular sink, all under the condition of wind blowing. The wind flow itself corresponds to a translation flow with velocity gradient. Influence of the ground is brought about by reflection of the potential flow.

The complete potential-theoretical model with the different singularities for calculating the recirculation flow velocities is illustrated in fig.4.

Since the velocity components are calculated from potential equations, the potential functions of different types of sources are enumerated here. For the sake of completeness the potential function of two-dimensional flows will also be given:

		two-dimensional	three-dimensional
(2)	point source	--	$\phi = -\frac{1}{4\pi}\cdot\dot{V}\cdot\frac{1}{r}$
(3)	line source	$\phi = \frac{1}{2\pi}\cdot\frac{\dot{V}}{l}\cdot\ln r$	$\phi = -\frac{1}{4\pi}\cdot\frac{\dot{V}}{l}\cdot\int_S \frac{1}{r}\cdot ds$
(4)	area source	$\phi = \frac{1}{2\pi}\cdot\frac{\dot{V}}{F}\cdot\int_S \ln r\cdot ds$	$\phi = -\frac{1}{4\pi}\cdot\frac{\dot{V}}{F}\cdot\iint_F \frac{1}{r}\cdot dF$
(5)	space source	$\phi = \frac{1}{2\pi}\cdot\frac{\dot{V}}{V}\cdot\iint_F \ln r\cdot dF$	$\phi = -\frac{1}{4\pi}\cdot\frac{\dot{V}}{V}\cdot\iiint_V \frac{1}{r}\cdot dV$

$\dot{V}$ stands here for the amount of source. l, F and V stand for the line, area and volume extension of the source and r stands for the distance between the inducing point of source and the point where the induced velocity may be found by differentiation of the potential function:

(6) $$u = \frac{d\phi}{dy} \quad , \qquad v = \frac{d\phi}{dz} \quad .$$

The velocity and its direction at any point of the y-z-plane results the vectorial sum of the components U_{ges} and V_{ges}. These consist of the induced velocity components of all singularities from the potential-theoretical model:

$$U_{ges} = U_1 + U_2 + U_3 + \ldots\ldots\ldots U_{10} + U_w$$

$$V_{ges} = V_1 + V_2 + V_3 + \ldots\ldots\ldots V_{10} \quad .$$

Limiting conditions that are necessary for the potential-theoretical calculation are the strenths of the sources and the geometrical dimensions of the model.

Half the sink-strength of a singularity has the same value as the velocity component that is induced vertically to its surface. Therefore the sink-strength of the jet is identical with double its inflow velocity. The distribution of the inflow velocities of the free

jet and of the wall jet are cited from [4] and illustrated in fig.5 and fig.6. The extension of the singularities no.7, 8 and 9 are determined by the lengths of separation of the wall jet. This is shown in fig.7 in its dependence on the wind velocity and on the nozzle Mach number.

Fig. 8 depicts the basic case of the secondary flow of a single propulsion jet. Here ambient air is sucked in by the engine inlet, by the free jet and by the wall jet in a calm. The flow into the engine inlet, positioned at the RB 162 about four nozzle diameters above the nozzle plane, is being reached by a point sink in the inlet plane and by a point source arranged two nozzle diameters below. The sink-distribution of the line sink of the free jet and the surface sink of the wall jet have been taken from test-readings on inflow velocities (fig.6, 7).

At a distance of 41 m from the point of impingement the wall jet detaches in an arc by thermic buoyant forces from the ground. At the point of separation the wall jet is represented by a cylinder source. The source distribution of the latter resembles that of a wall jet velocity-profile with its maximum value at the ground and zero at an altitude of 4 m. The volume flow that flows outwardly from the cylinder source must be equal to the flow that is injected by inlet, free jet and wall jet.

In fig. 9 the secondary flow field is overlayed by a wind flow, the velocity profile of which is cited from [4]. The engine inlet-flow, the free jet and the leeward area that is swept by the wall jet remain constant. On the other hand the line of separation of the wall jet running against the wind deforms into a semi-ellipse by the premature separation of the wall jet. The semi-ellipse has the large semiaxis perpendicular to the direction of the wind. The basal surface of the wall jet, the annular sink 8 and the cylinder source 9 take elliptic shape in both quadrants that are directed at the windflow. Correspondingly the source distribution of the singularities 8 and 9 becomes a function of the angle φ . In case of small angles the length of the wall jet is short and the volume that flows out of the point of separation is accordingly smaller than that in the case of big angles φ . Moreover the height of the cylinder source 9 also changes with variable φ . The height of the cylinder must always correspond with the actual wall jet thickness at different separation lengths.

3. CALCULATION OF THE RECIRCULATION TEMPERATURES

Now the calculation of the temperature distribution in the recirculation flow field is to be dealt with.

The axially symmetrical wall jet deflects from the ground along an arc at a calm because of the effect of the thermic buoyant forces. Further movement of the warm air in the atmosphere is determined only by the buoyant forces and by the injection effect of the propulsion jet. Kinetic forces however enforce the separation by wind-blast, the line of separation is then deformed into a semi-ellipse and the separated warm air cloud spreads further under the dominating influence of the wind flow. The mathematical calculation of the process is facilitated by the fact that the elliptical deformed line of separation (fig.4) runs near the middle section (y - axis) almost parallel to the x-axis. Compared with the axially symmetrical case the backblow of warm air on the line of symmetry in the recirculation flow

process may well be regarded as a two-dimensional process. The line of separation is being replaced by an infinitely long slit of variable width. From the latter hot gas emerges with overtemperature and with initial momentum. The spread of these two-dimensional hot gas jets in the atmosphere is - completely isolated from the above analysed recirculation problem - dealt with in chapter 3.1. Here velocity, temperature and width of the rising warm air flow are calculated disregarding the outer wind influences and the sink effect of the wall jet. In chapter 3.2 the results of this calculation are first applied to the recirculation flow.

3.1 TWO-DIMENSIONAL FLOW

It is started with the equations for the mass-, momentum- and heat-flow. x stands for the co-ordinate in the main flow direction (fig. 1o) y stands for the perpendicular co-ordinate while u and v stand for the corresponding velocity components.

Continuity equation:

$$(7) \quad \frac{\partial \rho \cdot u}{\partial x} + \frac{\partial \rho \cdot v}{\partial y} = 0$$

equation of motion:

$$(8) \quad \rho \cdot \left(\frac{\partial u}{\partial t} + u \frac{\partial u}{\partial x} + v \frac{\partial u}{\partial y}\right) = X - \frac{\partial P}{\partial x} + \mu \cdot \left(\frac{\partial^2 u}{\partial x^2} + \frac{\partial^2 u}{\partial y^2}\right)$$

energy equation:

$$(9) \quad \rho \cdot cp \cdot \left(\frac{\partial T}{\partial t} + u \frac{\partial T}{\partial x} + v \frac{\partial T}{\partial y}\right) = \lambda \cdot \left(\frac{\partial^2 T}{\partial x^2} + \frac{\partial^2 T}{\partial y^2}\right) \quad .$$

This equation system has to be reduced in the above case of a recirculation flow by certain hypotheses. So the calculation is based on a stationary flow. This certainly means a great simplification of this highly turbulent flow process. However the results show that the calculation with a stationary flow can determine the average flow parameters precisely enough. In the equation of motion the pressure- and friction element is neglected while the heat condition and the radiation are omitted in the energy equation. Furthermore the potential temperature Θ and turbulent fluctuating values are introduced.

In the recirculation flow the point of separation - where two gas flows, wind and a wall jet meet - is replaced by a line source with initial momentum and overtemperature.

No data exist so far about the velocity profile in such a two-dimensional "fountain", therefore it is very difficult to make any statement.

In the following a profile is therefore assumed in such a manner that the velocity inside the upwind is constant for an average velocity $u_m(x)$ and outside the upwind $u_m(x)=0$. A constant width $b(x)$ is thereby assigned to the upwind (fig. 1o).

The same considerations apply to the temperature profile. In spite of different exchange mechanisms for momentum and heat, in the considered case of the two-dimensional buoyant flow the ratio of the width

of the velocity profile to that of the temperature profile is set equal to 1. A rectangular profile therefore exists for calculation, with:

$$\left.\begin{aligned} &-b \leq y \leq +b \\ &u(x,y) = u_m(x) \\ &\theta'(x,y) = \theta'_m(x) \end{aligned}\right\} \quad x = \text{constant} \quad . \tag{10}$$

At the jet border $\overline{v}_b$ stands for the velocity with which the ambient air flows into the upwind. According to Morton-Taylor-Turner [2] the inflow velocity is proportional to the average flow velocity in the x-direction with a constant proportionality factor.

$$\overline{v}_b = \alpha \cdot u_m \quad . \tag{11}$$

The integrated equation system now reads (the integration is described in [4]:

$$\frac{d}{dx} u_m \cdot b = \alpha \cdot u_m \tag{12}$$

$$\frac{d}{dx} u_m^2 \cdot b = g \cdot b \cdot \frac{\theta'_m}{\theta_a} \tag{13}$$

$$\frac{d}{dx} g \cdot b \cdot u_m \cdot \frac{\theta'_m}{\theta_a} = -u_m \cdot b \cdot g \cdot \frac{1}{\theta_a} \frac{d\theta_a}{dx} \quad . \tag{14}$$

The recirculation flow at consideration represents an initial-value problem. For x = 0 are valid:

$$\left.\begin{aligned} b &= b_o \\ u_m &= u_{m_o} \\ \theta_m &= \theta_{m_o} \end{aligned}\right\} \quad . \tag{15}$$

In order to obtain independent solutions from the initial values it is well suited to introduce dimensionless values:

$$\xi = \frac{\alpha \cdot x}{b_o} \tag{16}$$

$$\eta = \frac{b}{b_o} \tag{17}$$

$$\varphi = \frac{u_m}{(b_o \cdot g)^{1/2}} \cdot \left[\frac{\alpha}{\left(\frac{\theta'_m}{\theta_a}\right)_o} \right]^{1/2} \tag{18}$$

$$\lambda = \left(\frac{\theta'_m}{\theta_a}\right) \Big/ \left(\frac{\theta'_m}{\theta_a}\right)_o \tag{19}$$

(20) $$\gamma = \frac{1}{\Theta_a} \cdot \frac{d\Theta_a}{dx} \cdot \frac{b_o}{\alpha \cdot \left(\frac{\Theta'_m}{\Theta_a}\right)_o} \quad .$$

The unknown parameters are now:

η parameter for the width of the upwind flow

φ parameter for the velocity of the upwind flow

λ parameter for the temperature of the upwind flow

γ parameter for the temperature gradient, which generally is presupposed.

With the substitution

(21) $$V = \eta \cdot \varphi$$

(22) $$W = \eta \cdot \varphi^2$$

(23) $$Z = \lambda \cdot \eta \cdot \varphi$$

or

(24) $$\lambda = \frac{Z}{V}$$

(25) $$\varphi = \frac{W}{V}$$

(26) $$\eta = \frac{V^2}{W}$$

one arrives at the final differential equation system of the infinite line source with initial momentum and buoyant force:

(27) $$V \frac{dV}{d\varphi} = W$$

(28) $$W \frac{dW}{d\varphi} = Z \cdot V$$

(29) $$\frac{dZ}{d\varphi} = -\gamma \cdot V \quad .$$

Initial terms:

(30)
$$\varphi = o$$
$$V_o = \varphi_o$$
$$W_o = \varphi_o^2$$
$$Z_o = \varphi_o \quad .$$

General solutions for the differential equation system may be gained by a numerical integration according to the Runge-Kutta-method. Fig.11.

The overtemperature in the upwind decreases in correspondence with a hyperbolic function. The smaller decrease of temperature at high initial velocities enforce stronger buoyant forces in the rising cloud. For that reason the constant final velocity is also greater at high φ_o-values. At great φ_o-values the upwind reaches a certain distance from the

source sooner than at slow initial velocities. It has less time for turbulent mixing with the ambient air; therefore at the same initial temperature values the faster warm air flow always has higher temperatures.

3.2 UPWIND FLOW IN THE RECIRCULATION FLOW FIELD

The behaviour of the upwind flow in the recirculation flow field is now to be examined. At the point of separation of the wall jet the warm air flows vertically upwards, it is seized by the wind, is deflected in the direction of the wind flow and then blown away. The warm air cloud thereby sweeps over the encountering wall jet, it is sucked in by the sink effect and it is absorbed to a great extent. Ambient air cannot enter the underside of the hot gas cloud then anymore. In order to allow for a theoretical description of this complicated flow process, the recirculation process will be simplified for further considerations. This will be done in such a way that the injection effect of the wall jet on the underside of the warm air flow is to be neglected. The recirculation flow will then be regarded as an upwind flow with initial momentum that has been deflected in direction of the wind.

It is being assumed that the mechanism of the turbulent mixing of the warm air cloud with the ambient air with influence of wind is equal to that without wind influence. This certainly is the case with the low wind velocities under consideration. After equal periods of time the conditions of the warm air cloud that rises in calm air are equal to those in the cloud blown away by the wind.

With y standing for the co-ordinate in the direction of wind, x for the corresponding vertical co-ordinate, u_m for the average wind velocity (fig.12) one has

(31) $$dy = w\, dt \quad .$$

If w is taken as a constant value, then - with the co-ordinates as stated in fig.12 above - one has

$$y = w\, t \quad .$$

The time the vertical rising cloud takes from the source to the co-ordinate x' is calculated from:

(32) $$u_{m(x)} = \frac{dx}{dt}$$

$$dt = \frac{dx}{u_{m(x)}}$$

(33) $$t = \int_0^{x'} \frac{dx}{u_{m(x)}} \quad .$$

In the same duration of time the cloud that is blown with the wind velocity w reaches the co-ordinate y'

(34) $$y' = w \cdot \int_0^{x'} \frac{dx}{u_{m(x)}} \quad .$$

Thereby every point y in direction of the wind is co-ordinated to a condition of the vertical rising cloud without wind. For practical calculation the recirculation flow picture fig. 9 is used to determine the recirculation velocity $w_{(y)}$ and the time period t, that is needed by a particle of air to proceed from the point of separation R on the passage s with the recirculation velocity $w_{(y)}$ to the engine on the z-axis.

$$t = \frac{w_{(y)}}{s} \quad . \tag{35}$$

Within this period a thermic cloud that rises with the velocity $u_{m(x)}$ covers the vertical length of passage x'

$$x' = \frac{u_{m(x)}}{t} \quad . \tag{36}$$

At this point it has the same overtemperature as the recirculation flow at the plane of the propulsion unit. Thereby the recirculation problem is reduced to the spreading process of the vertical rising two-dimensional upwind cloud as calculated in chapter 3.1.

4. EXPERIMENTS

At the Bodeneffekt Versuchsanlage of the DFVLR Institut für Luftsaugende Antriebe at Braunschweig the investigations about recirculation took place with two lift engine models of different height. The test set up is described in detail in [4] and illustrated in fig.13.

The velocity measurements in a recirculation flow field of lift engines demands a great input of measuring technique. This is due to the highly turbulent warm air flows, the velocity- and temperature fluctuations of which can surpass even the value in the main flow direction. The dynamic pressures of the recirculation flow are in the order of only a few mm column of water; therefore pitot tubes are unsuitable for the measuring of velocity.

Temperature-compensated hot film probes were used to determine the velocities of the recirculation flow field at various points on the y-z plane (fig.16). The flow directions at the measuring points were specified with wool threads and light-intersection-photos (fig.2o). The light-intersection-photos depict the physical process of recirculation particularly well. In fig.18 the exhaust jet of the model-engine has been inked; on the other hand the wind remains without colour. In fig.19 contrast powder was blown into the lowest layer of the wind flow; here the jet of the exhaust gas was left invisible. As may be read from the photos the shape of the boundary line between wall jet air and wind is different with both inking methods. The boundary line took a higher arc with the inking of the wall jet than with that of the wind. Reason for this is the turbulent mixing of the inked air with the colourless air. The visible boundary line represents the outmost course of the turbulence-conglomerates that proceed from the inked flow and have entered the dark flow. The visible boundary line with the colourless wind that has been produced by inking of the wall jet is of great evidence for investigation on recirculation. It describes the maximum height, the air - heated by the engine jet - can reach. If the engine inlet lies below this line a rise in temperature due to recirculation must be considered for. If the inlet

lies above this line only cold ambient air is being sucked in. The measuring of this temperature-boundary line is described next.

The temperature measurment in the recirculation flow field and in the engine inlet was conducted with o,5 mm NiCr-Ni-thermocouples. In fig.21 the temperature is plotted as a function of the height. From this graph the boundary line between the recirculation flow heated by the engine jet and the wind sweeping over it with ambient temperature can best be taken. This recirculation boundary line has been defined as the position where the temperature profile has dropped to 1o to 2o% of its maximum value. This boundary line is identical with the visible border between the inked wall jet air and the dark wind air as can be seen on the light-intersection-photos (fig.2o). It may therefore be determined without temperature measurements only by inking of the engine jet and by illuminating with the light plane projector.

The engine inlet temperatures were measured with thermocouple at the inlet plane. Fig.23 illustrates the temperature plot as registered over a period of 3o seconds. Contrary to suction air temperatures that occur with lift engine arrangements with accompanying fountains, the temperature distribution in the compressor inlet plane with wind recirculation is quite constant. Only a small rise in temperature can be registered towards the windward side.

5. RESULTS

Summarizing it should be emphasised that only a stationary laminar isothermic flow field is calculated with a potential-theoretical model. The flow field is not identical with the real highly turbulent and heated recirculation flow. Conclusions cannot be drawn on turbulent mixing processes, e.g. the determination of the boundary line between warm wall jet air and a cold wind flow. However the investigations confirm that average turbulent velocities and their directions in the recirculation flow field correspond with those velocities that are calculated theoretically. By way of the mathematical method one is quite capable to determine the main flow that is important for a comprehension of the recirculation process and that is taken as basis for the complicated flow field. Also the calculation can distinctly show the most influential parameters in the flow field.

In fig.22 the measured temperatures of the recirculation cloud at the plane of the centre axis of the engine are compared with the theoretical results of chapter 3. The calculation results correspond very well with the measured data. The calculated Θ'_m-values are average values of the temperature profile. On the other hand the data measured resemble temperatures at the profile maximum and are therefore slightly higher.

It has thus been proved that the above presented theory is capable of giving quite exact results about the recirculation temperature that occurs in the engine inlet.

In fig.24 and 25 diagrams have been drawn for practical use. From these the results of the recirculation theory may be taken directly for the parameter one is interested in. With the help of fig.24 it may be judged whether the engine configuration under consideration is in danger of recirculation. In this diagram the upper borders of the recirculation clouds at the plane of the centre axis of the engine - as visible on the light-intersection-photos - have been plotted as a

function of the wind velocity. Engine inlets that have been arranged high above the ground are not so susceptible to recirculation than those with inlets situated lower down. The temperature boundary line can exceed highly arranged engine inlets only at small wind velocities, thereby endangering these configurations with recirculation. Any influence of the nozzle temperature on the shape of the boundary line could not be determined. If at a certain configuration the point of intersection from the normalized ground distance z/D of the inlet and of the wind velocity lie below the plotted curve with the specified engine parameters (nozzle Machnumber M_o and H/D) then one has a lift engine arrangement that is susceptible to recirculation.

From fig.25 the occuring rise in temperature can now be taken. As the case may be - if one has a configuration with the jet core impinging on the ground, or not - one carries on in the right column from the nozzle Mach number M_o up to the prevailing wind velocity w. From this ordinate value a straight line is drawn in the left half of the diagram to the origin. Now as a function of the nozzle temperature the average inlet temperature may be read.

6. CONCLUSIONS

In detail the physical process of wind recirculation has been dealt with. This type of recirculation flow will more often occur with future VTOL-aircrafts. Wind recirculation is favoured by modern trends to develop jet engines with even bigger-volumed jets with lower specific momentum.

The average velocities of the three-dimensional recirculation flow field, as produced by wind, were calculated by potential theory for a single lift engine impinging vertically on the ground. With the help of the spreading laws of warm air clouds the average recirculation temperatures were determined, verified and confirmed by model tests. The velocities and temperatures present in the engine inlet plane may be predicted precisely enough with the above described method. For this calculation only the data of the wind velocity, the geometry of the lift engine and the nozzle conditions of the exhaust gas jet are needed. The wind recirculation may be treated as a potential flow, because it was proved that the kinetic forces occuring in the secondary flow field always exceed the thermic forces by more than one tenth power.

The investigations on the recirculation flow field have led to the following results:
No recirculation will occur at a single VTOL-propulsion jet without wind blowing.

A suitable criterion for judgement whether warm air can reach the engine inlet by a recirculation flow is given by the light-intersection-method. Thereby the shape of the temperature boundary is made visible.

The recirculation velocities induced by a rotation-symmetrical exhaust-gas jet differ only very slightly from the local wind velocities that impress themselves dominantly on the entire flow field.

Wind recirculation to the engine inlet is favoured by:

small wind velocity
engine inlet arranged near to the ground
high exhaust gas temperature
low exhaust gas velocity.

REFERENCES

[1] Morton, B. — Forced Plumes, Journal of Fluid Mechanics, Vol. 5, Part 1, 1959, S. 151-163

[2] Morton, B. Taylor, G. Turner, J. — Turbulent Gravitational Convection from Maintained and Instantaneous Sources, Proc. Roy. Soc. London, Vol. 234, A 1956, S. 1-23

[3] Murgai, M. Emmons, H. — Natural Convection above Fires, Journal of Fluid Mechanics, Vol. 8, Part 1, 196o, S. 611-624

[4] Schwantes, E. — Das Rezirkulationsströmungsfeld eines VTOL-Hubtriebwerks, DLR FB 72-5o, Juli 1972

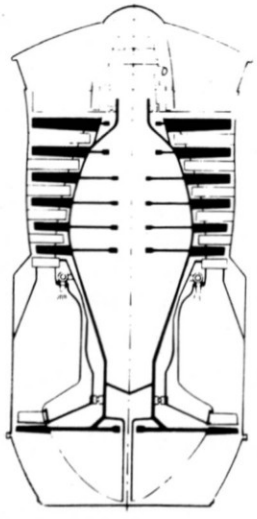

Fig. 1 Lift engine Rolls Royce RB 162

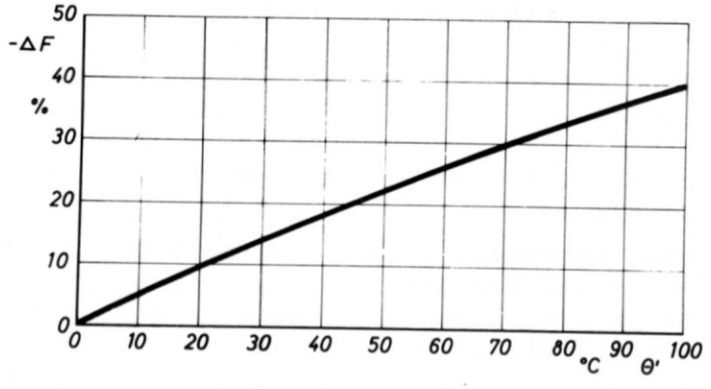

Fig. 2 Thrust-loss of the RB 162 as function of increase of temperature in the compressor inlet.

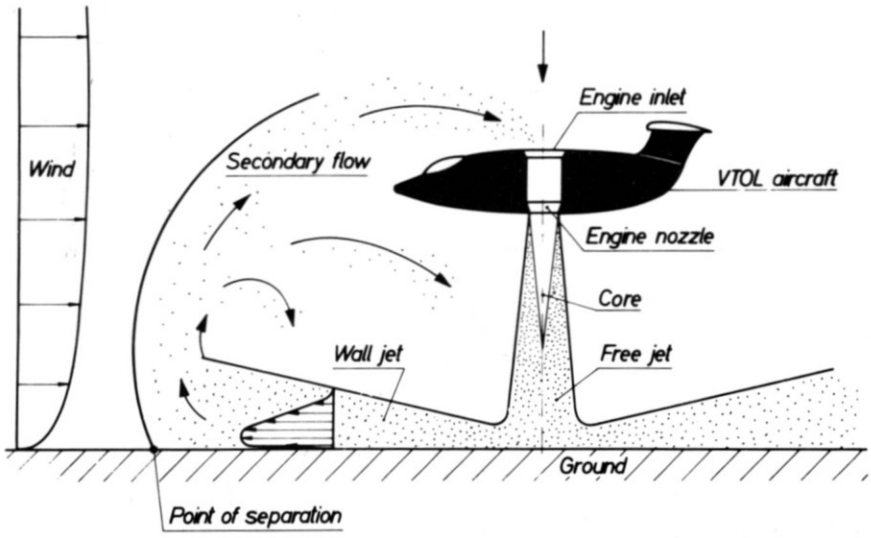

Fig. 3 Wind-recirculation of a VTOL-aircraft.

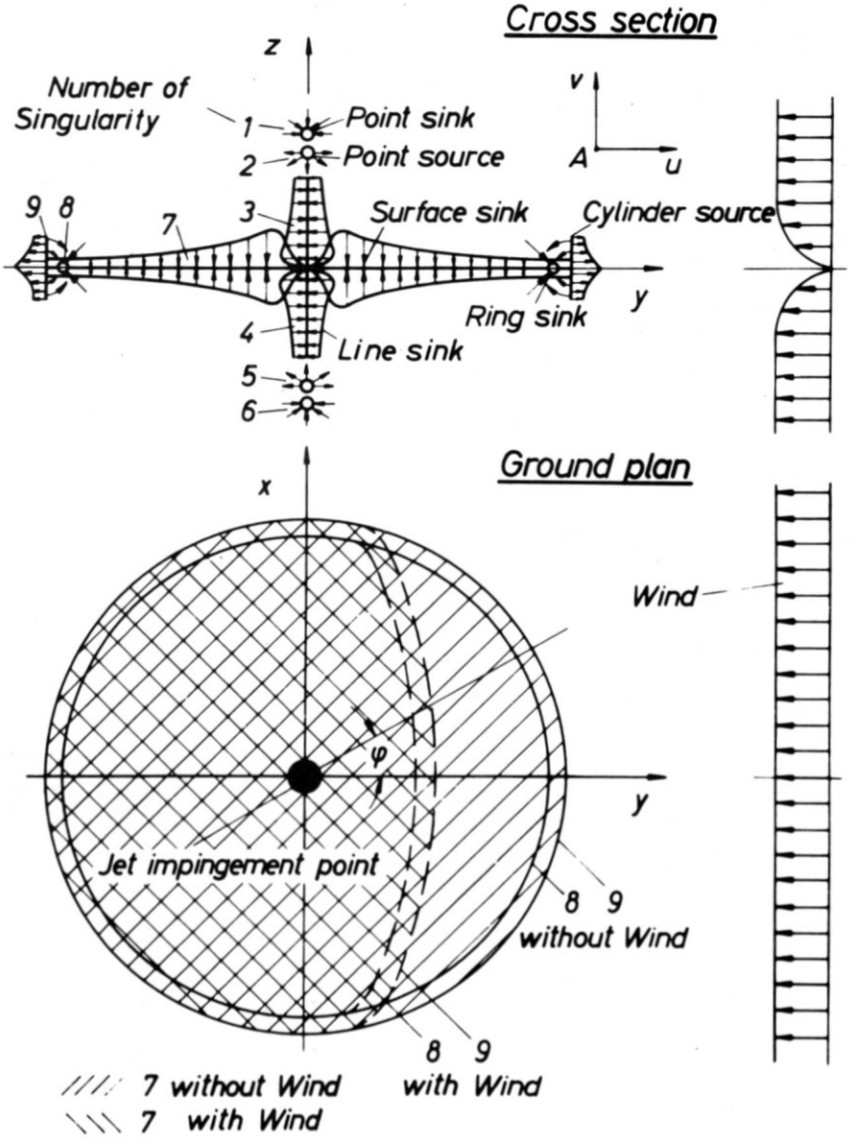

Fig. 4 Potential theoretical model

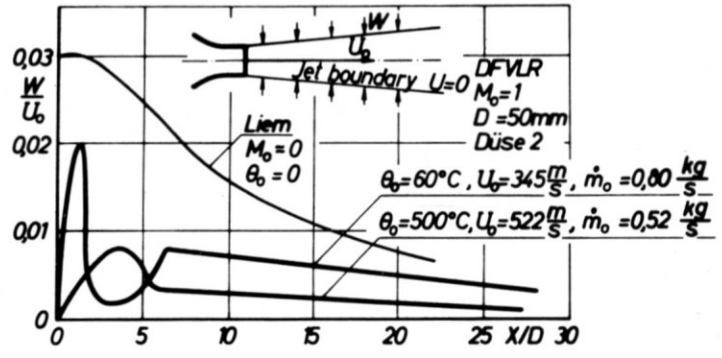

Fig. 5 Inflow velocity into the free jet, influence of temperature and Mach number.

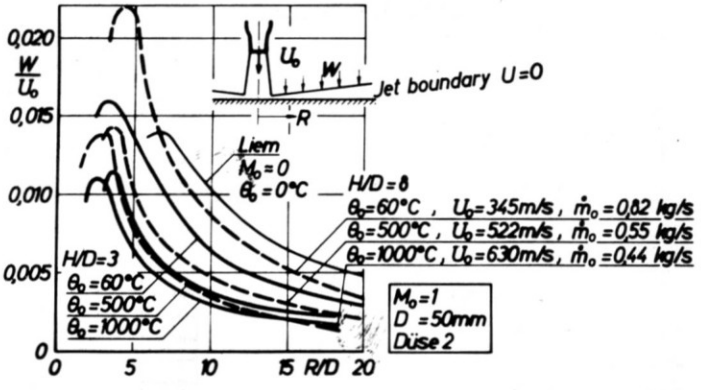

Fig. 6 Inflow velocity into the wall jet, influence of temperature and H/D.

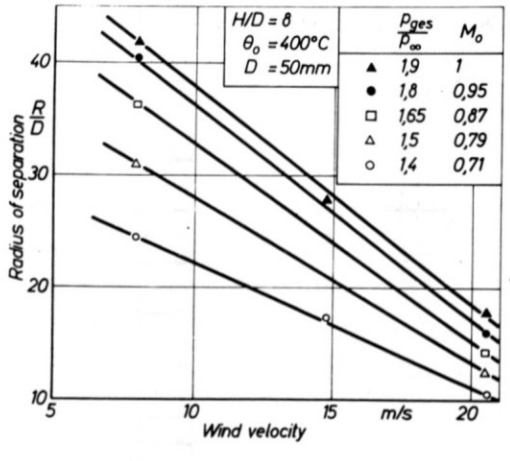

Fig. 7 Radius of separation of the wall jet, influence of nozzle Mach number.

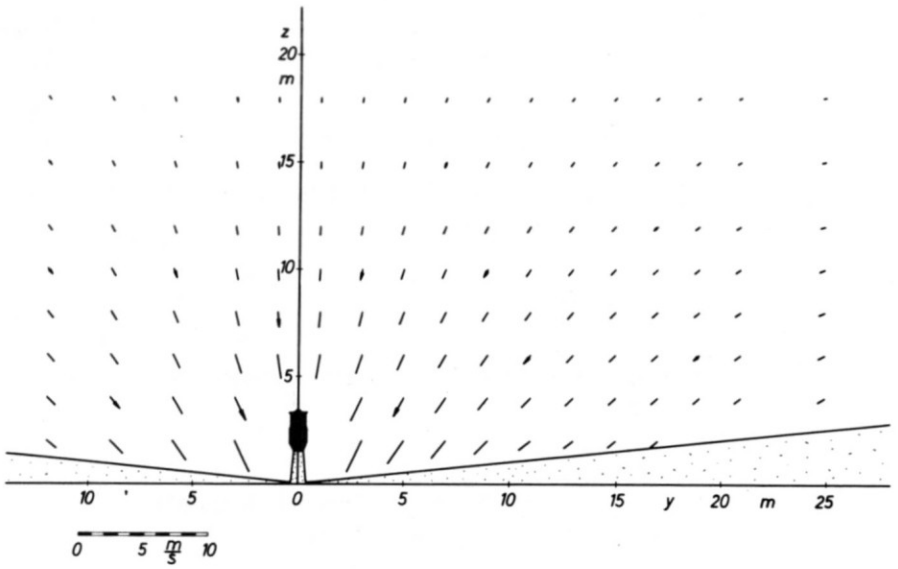

Fig. 8 Calculated velocities in the y-z plane of the secondary flow field of the lift engine RB 162-31, without wind, $M_o = 1$, $H/D = 3$.

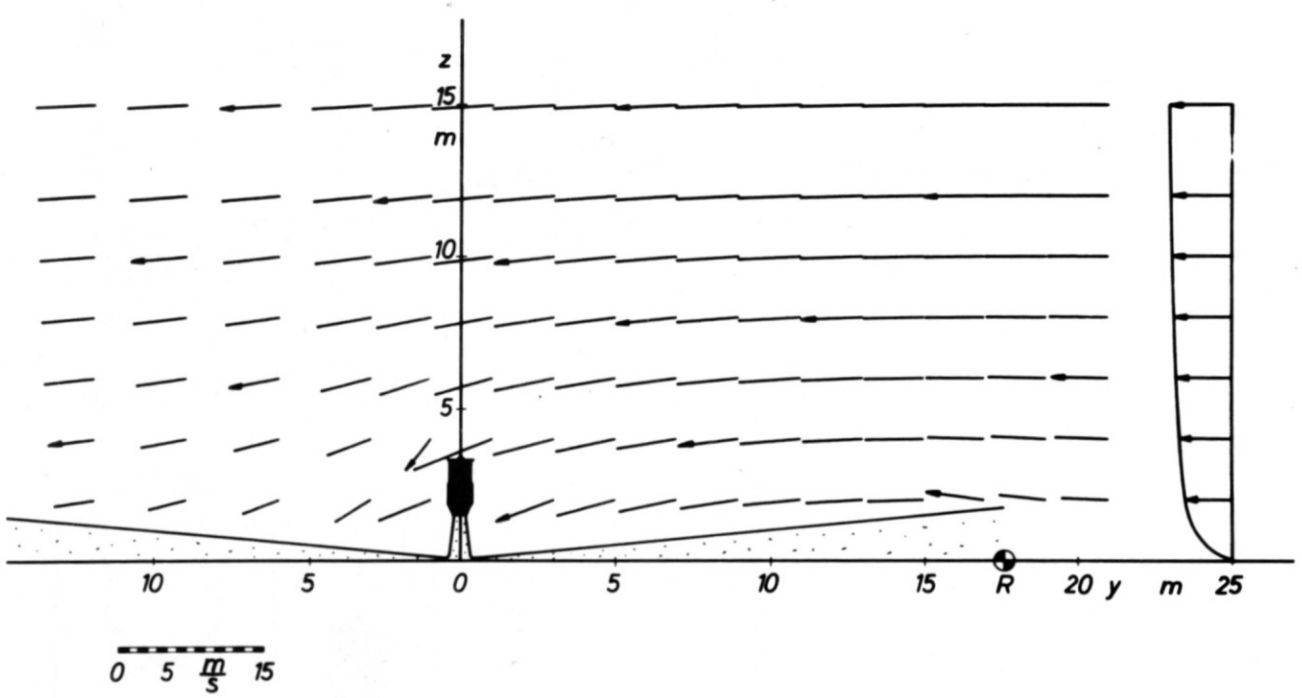

Fig. 9 Calculated velocities in the y-z plane of the recirculation flow field of the lift engine RB 162-31 $M_o = 1$, $H/D = 3$, $W = 5 \frac{m}{s}$.

◓ radius of separation of the wall jet

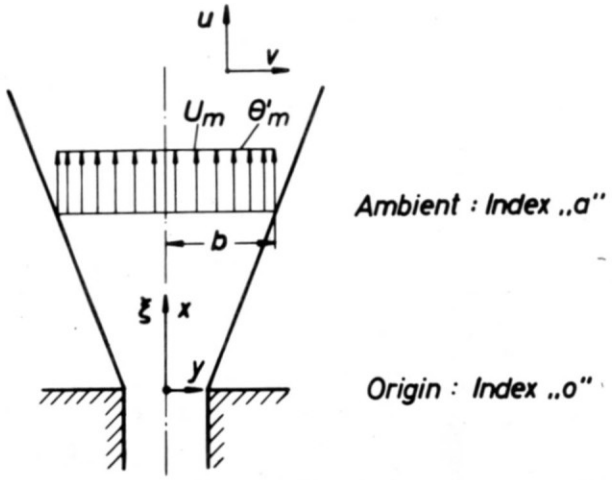

Fig. 10 Co-ordinate system of a plane source of warm air.

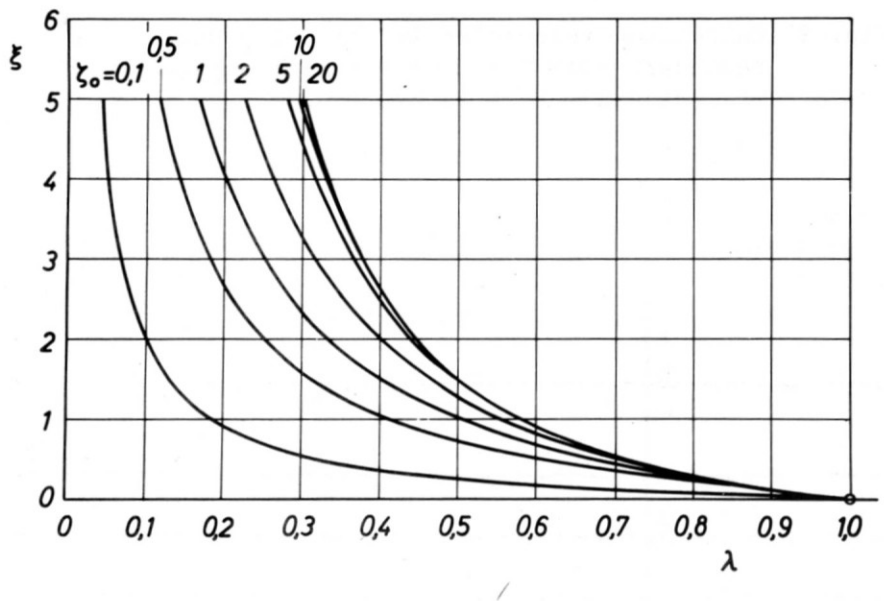

Fig. 11 Temperature of a plane upwind as function of the height.

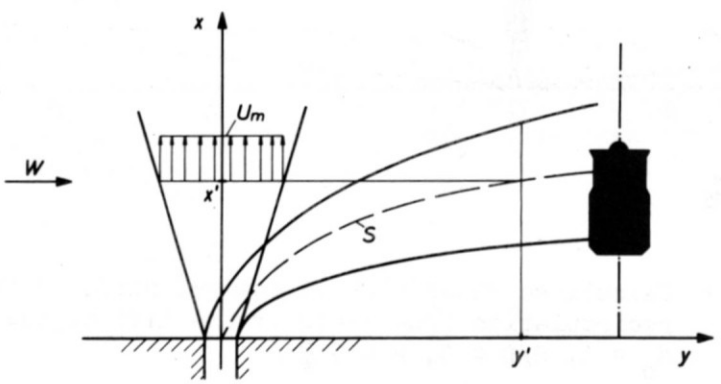

Fig. 12 Co-ordinate system of a plane source blown against by a cross-wind.

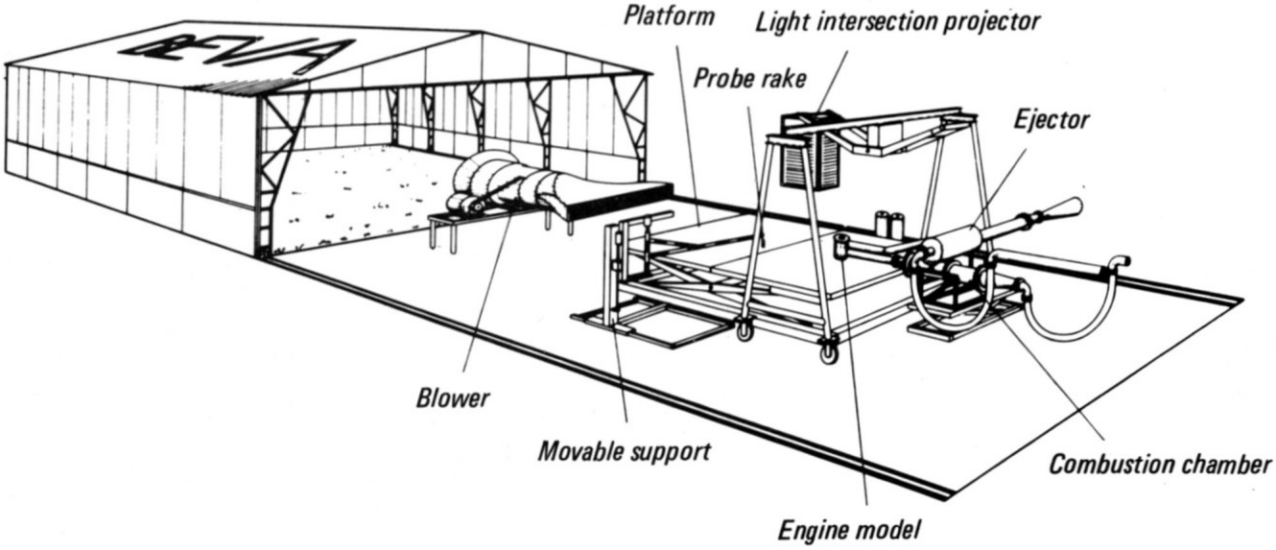

Fig. 13 Ground effect facility

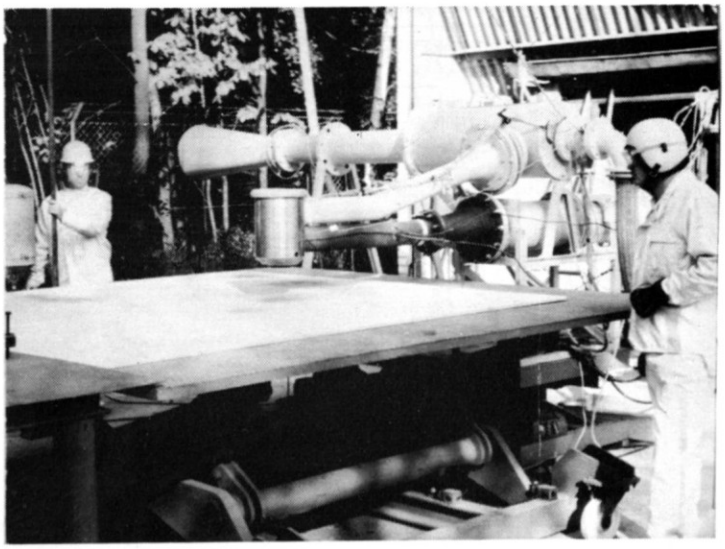

Fig. 14

Ground effect test set-up with model engine No. 1.

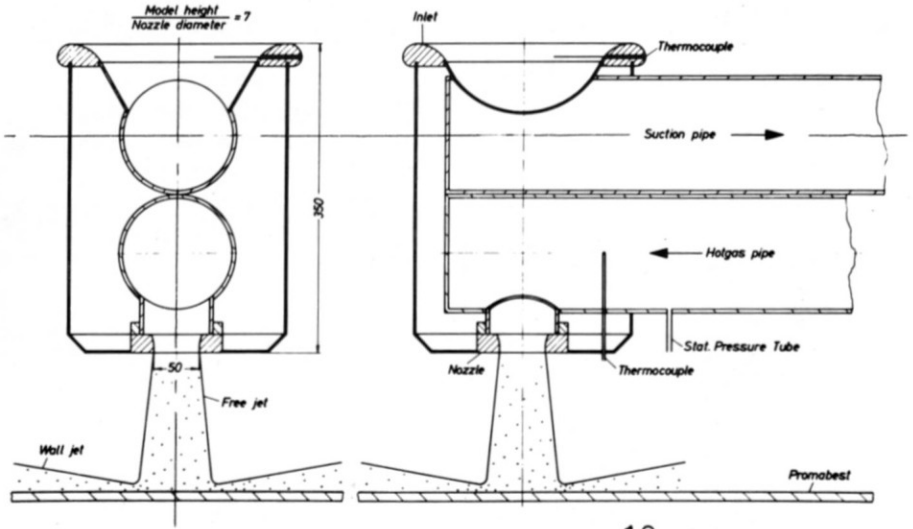

Fig. 15

Engine model No. 1.

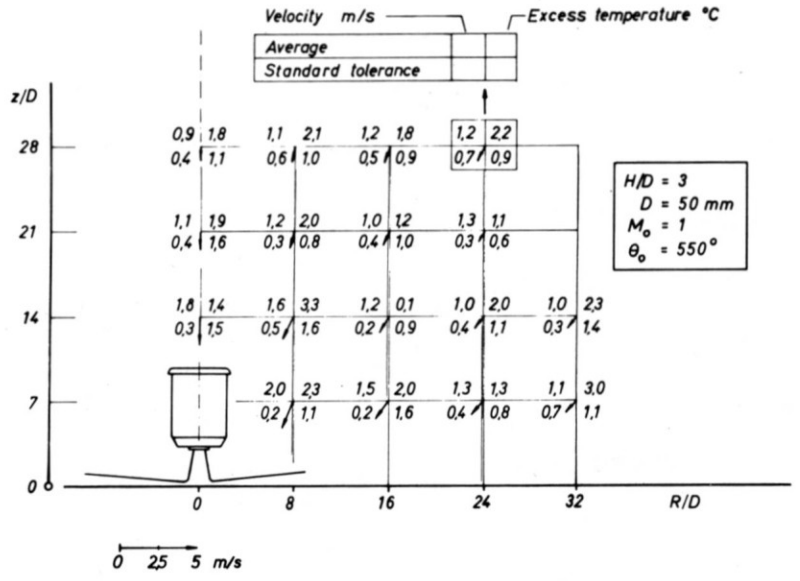

Fig. 16

Velocities and overtemperatures in the y-z plane of the secondary flow field, without wind.

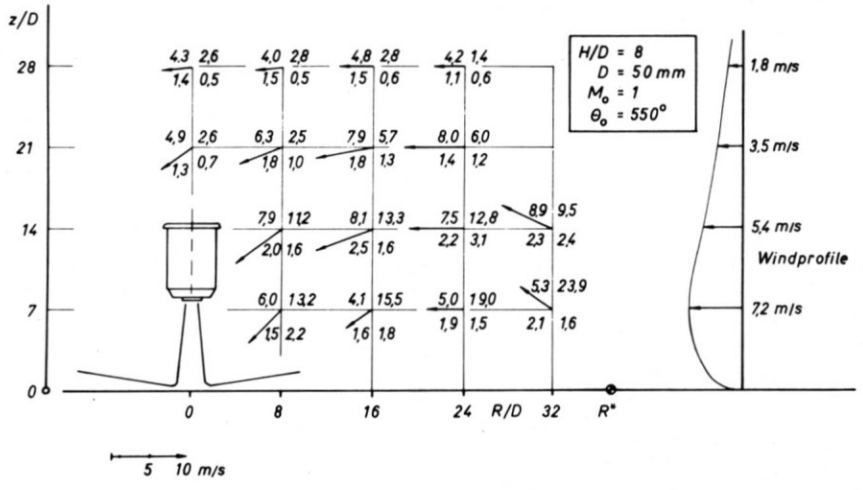

Fig. 17

Velocities and overtemperatures measured in the y-z plane of the recirculation flow field.
R*: Radius of separation of the wall jet

Fig. 18 Light-intersection-photograph of the separationof the wall jet, made visible by inking of the engine jet.

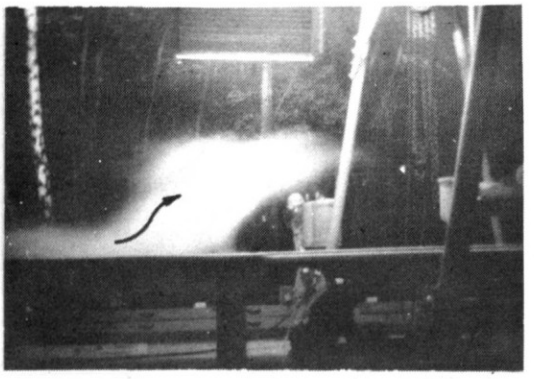

Fig. 19 Light-intersection-photograph of the separation of the wall jet, made visible by inking of the wind $M_o = 1$, $H/D = 3$, $\theta_o = 550\ ^oC$, $w_o = 8\ \frac{m}{s}$.

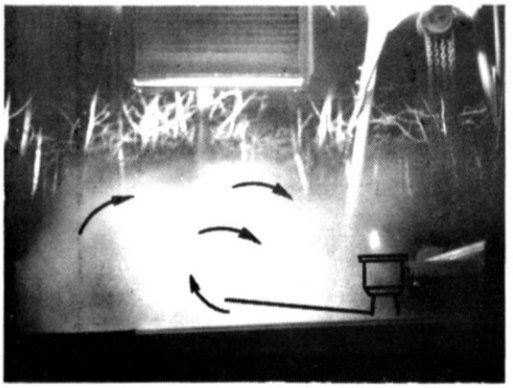

Fig. 20

Light-intersection-photograph of the recirculation flow field, configuration of fig. 19.

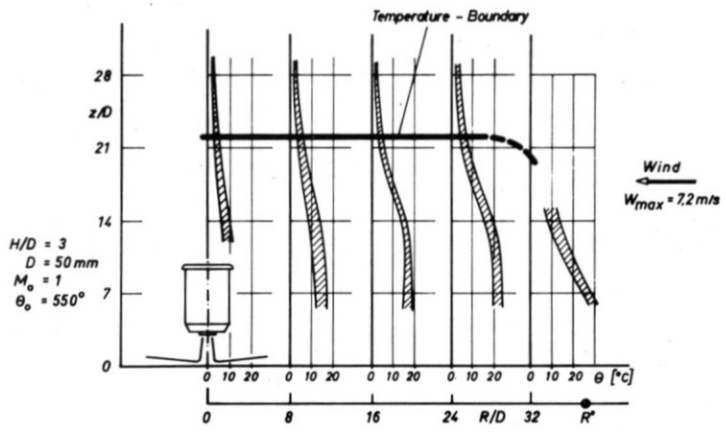

Fig. 21

Distribution of overtemperature in the recirculation flow field, H/D = 3, shaded section: Width of scattering of test data.

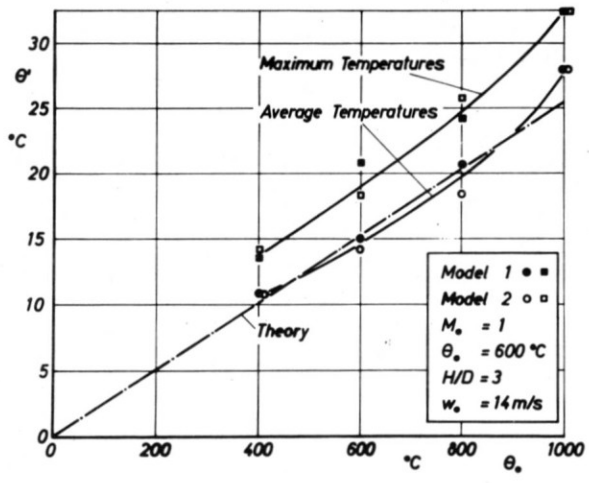

Fig. 22

Calculated and measured increases of temperatures in the compressor inlet as function of the exhaust gas jet temperature.

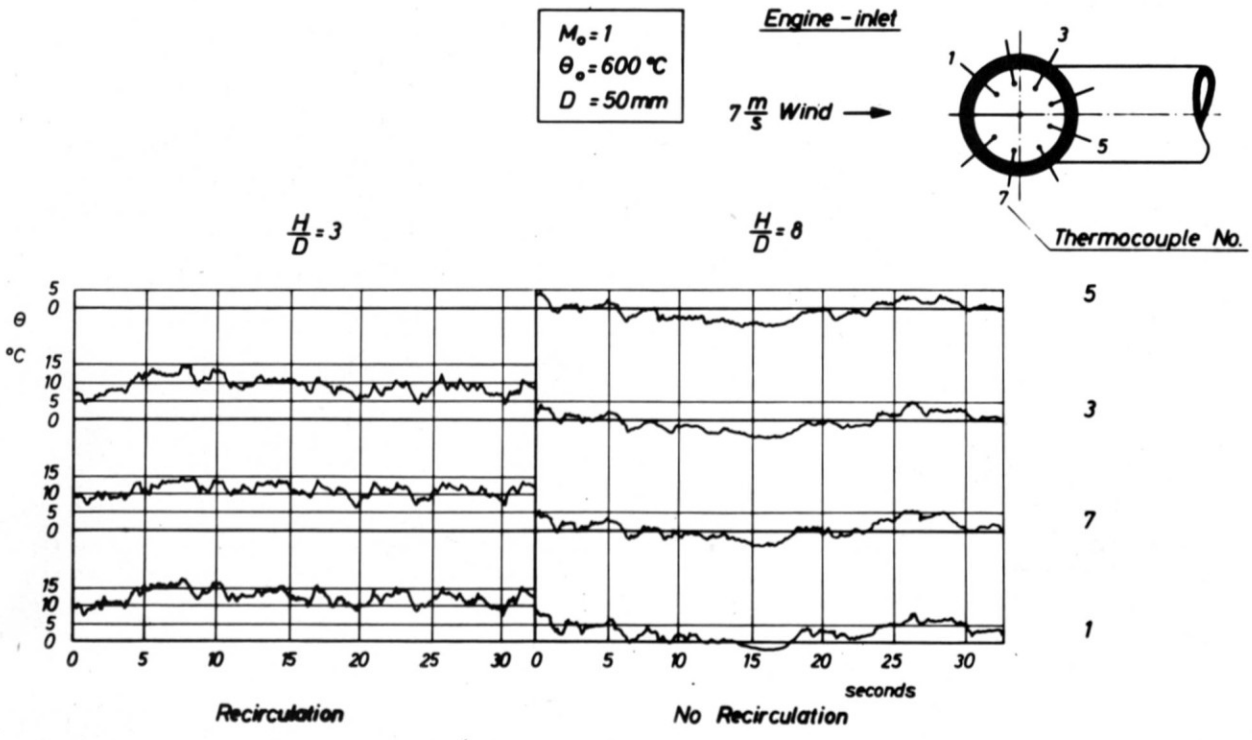

Fig. 23 Fluctuations of temperature in the engine inlet.

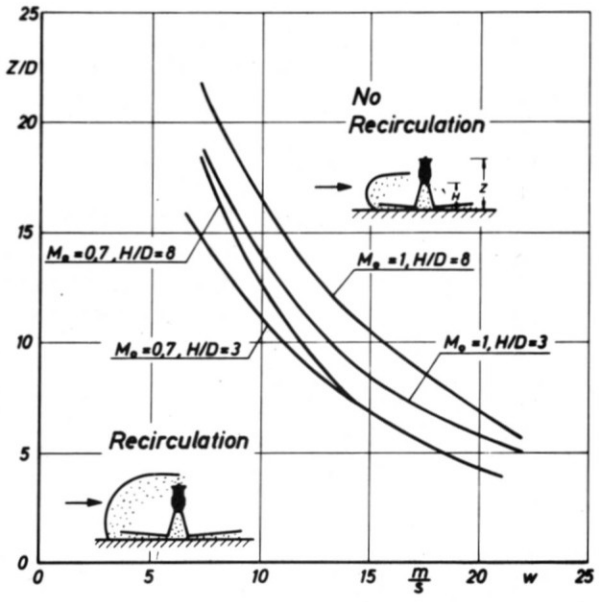

Fig. 24 Height of boundary line of temperature on the centre axis of the jet engine.

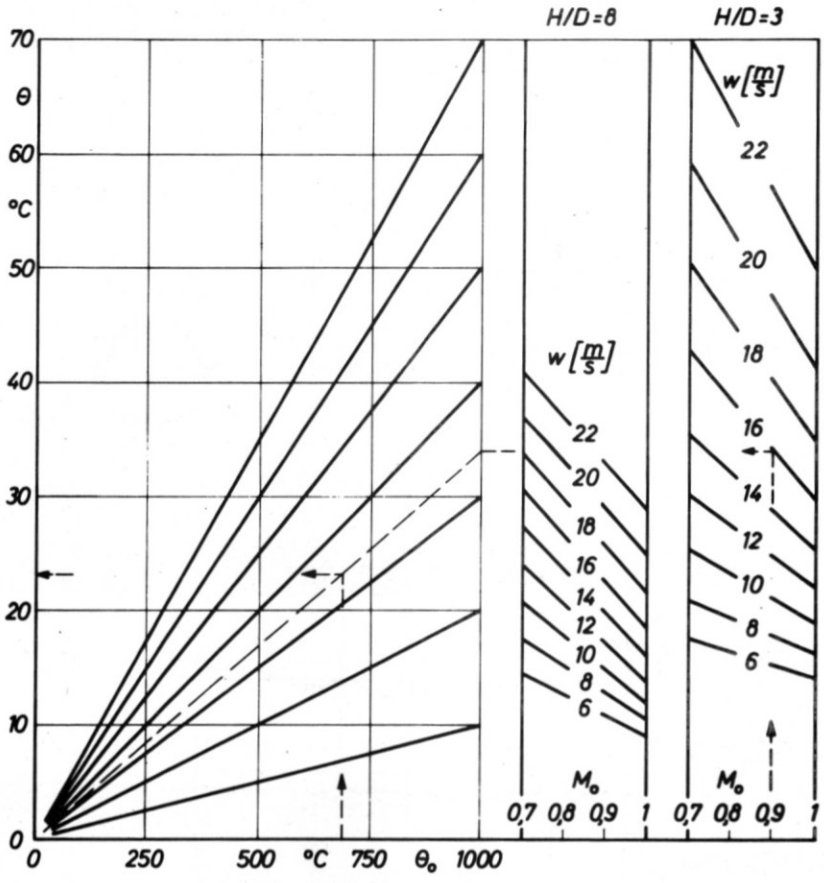

Fig. 25 Increase of temperature in the engine inlet produced by wind recirculation as function of M_o, W, ϑ, H/D.